

Effect of excited states on the ionization balance in plasmas via the enhancement of ionization and recombination rate coefficients

Kitae Lee and Dong-Eon Kim

Physics Department, Pohang University of Science and Technology, San 31 Hyoja-Dong, Nam Ku, Pohang, Kyungbuk 790-784, Korea

(Received 20 November 1998; revised manuscript received 22 March 1999)

The effect of excited states on the effective ionization and recombination rate coefficients for the ground states was investigated analytically and by computer simulation. The calculation was done for carbon ions. The results using carbon ions show (1) the contribution from excited states to ionization rate coefficients becomes significant even at an electron density as low as 10^{15} cm^{-3} and saturated from around $N_e \approx 10^{20} \text{ cm}^{-3}$; (2) the lower the electron temperature, the larger the contribution; (3) in the case of recombination rate coefficients, there is still a non-negligible contribution from excited states even at a very low electron density of 10^{10} cm^{-3} , where the contribution has been considered negligible; (4) this contribution to the recombination rate coefficients increases linearly with the electron density; (5) the enhancements of the ionization and recombination rate coefficients increase as N_e increases and are saturated to the same value at higher densities; (6) there exists a region of temperature and density where the recombination is effectively hindered. Some of the behaviors of the ionization and recombination rate coefficients in the extreme regions of a very low and high electron density were analytically understood. The calculated ionization and recombination rate coefficients for carbon ions, including the effect of excited states, were used in a one-dimensional magnetohydrodynamic code for the calculation of the ionization balance of carbon ions in a Z-pinch carbon plasma and the gain of C VI H $_{\alpha}$ (18.2 nm) line. The significant change in the evolution of the ionization balance was observed. The rapid depletion of C VII ions by the increased recombination rate reduces the gain significantly by a factor of ~ 3 compared to the case where the contribution from excited states was neglected. Such calculations can be done for other ions. The characteristics found for carbon ions are generic and applicable to other ions.

[S1063-651X(99)05008-4]

PACS number(s): 52.25.Jm, 42.55.Vc, 52.65.Kj

I. INTRODUCTION

Laboratory high density and temperature plasmas have practical applications which often demand the better understanding of the spectroscopic properties of such plasmas. Such demands have attracted research on atomic properties of dense plasma in astrophysics and laboratory plasma experiments [1]. One of the important properties to be understood is the contribution from excited states to the ionization balance.

The knowledge of the ionization balance is crucial for characterizing the spectroscopic properties of plasma because it determines the emission and absorption spectrum of the plasma. Chemical reactions in plasmas will be also significantly affected by the degree of ionization. The ionization balance has been calculated, considering atomic processes only between ground states of ionization stages. The underlying assumption is that the populations of ground states are far larger than those of excited states. This is no longer true at the high density region where the populations of excited states can be good fractions of ground-state populations. The present study shows that even at low density region where the populations of excited states are small compared to that of a ground state, excited states can still make a non-negligible contribution, especially in the recombination process.

X-ray laser study is one of the areas of research where the contribution from excited states can be important. At high plasma density relevant to x-ray laser experiments, in addition

to direct ground-to-ground ionization and recombination processes, indirect multistep processes involving excited states become significant. The electron-collisional recombination pumping scheme using an H-like or Li-like ion for the development of soft x-ray lasers [2–6] requires a plasma cooling rate faster than the recombination rate of fully stripped ions to H-like ions or He-like ions to Li-like ions. In a Z-pinch plasma for the development of soft x-ray lasers, the adiabatic expansion which was shown to play a main cooling role [7] are greatly affected by the rising and falling time of plasma current. Hence, the accurate estimate of the recombination rate becomes important, when one designs a pumping system for an x-ray laser.

Low-temperature and density plasmas have been used in science and industry. The application of such plasmas especially in semiconductor processing has been very successful and their roles become increasingly important. As better and tighter control of such plasmas are being required, research efforts have recently been increased toward better understanding of the characteristics of these plasmas [8,9]. In this vein, the contribution from excited states to the ionization balance, which has been considered negligible, is certainly an area to be understood.

A simulation code for the evaluation of the collisional-radiative (CR) ionization and recombination rate coefficients [10] which include the contribution from excited states was developed (Sec. II). The screened hydrogenic model [11] for the structure of energy states was used. By using the screened hydrogenic model, the calculation can be done for the wide range of elements with a reasonable accuracy.

While in this study the calculations were done for carbon ions and the conclusions were drawn with respect to them, the calculation for other ions can be readily done and conclusions made in this paper are generic and applicable to other ions. The general behavior of the calculated CR rate coefficients for carbon ions (Sec. III) and their effect on the ionization balance (Sec. IV) will be discussed.

II. CALCULATIONAL MODEL

The populations of excited states in the q th ionization stage are evaluated by the following set of the rate equations in the collisional-radiative model:

$$\begin{aligned} \frac{d}{dt}N_i^q = & -N_i^q \left[N_e S_i + N_e \sum_{j \neq i} C_{ij} + \sum_{j < i} A_{ij} \right] + N_e \sum_{j \neq i} N_j^q C_{ji} \\ & + \sum_{j > i} N_j^q A_{ji} + N_1^{q+1} N_e (N_e \alpha_i^{3b} + \alpha_i^{rr}), \end{aligned} \quad (1)$$

where N_i^q is the population of the i th state in the q th ionization, N_1^{q+1} the population of the ground state in the $(q+1)$ -th ionization stage, N_e the electron density, S_i the electron-collisional ionization rate coefficient of the i th state, C_{ij} the electron-collisional excitation (deexcitation) rate coefficient from the i th to j th state, A_{ij} the radiative transition rate from the i th to j th state, and α_i^{3b} and α_i^{rr} are the three-body and radiative recombination rate coefficients from the ground state of the $(q+1)$ -th ionization stage to the i th state, respectively.

This time-dependent rate equation is usually coupled with hydrodynamic equations of a plasma. If the relaxation times of excited levels are much shorter than the time scale of hydrodynamic variation for the range of plasma temperature and density under interest, it is sufficient to express the excited level populations in steady state as a function of ground level populations assuming that they reach a steady state. However, since the relaxation times of ground levels are in general, comparatively slow, it is solved time dependently. This is the quasi-steady-state (QSS) approximation. McWhirter *et al.* [12] analyzed the QSS approximation in detail and presented the valid range of electron temperature and density for hydrogenic ions. The validity of the QSS approximation in the plasma investigated in this paper is discussed in detail in Sec. IV. Under this approximation, dN_i^q/dt for the excited states can be put equal to zero except for ground state: $dN_i^q/dt=0$ for $i>1$. Then Eq. (1) can be rewritten in a matrix form as

$$D \cdot \vec{\rho} = \vec{b}^0 + N_e \rho_1 \vec{b}^1, \quad (2)$$

where

$$D_{ij} = \begin{cases} -N_e C_{ij}^{de} & \text{if } i > j \\ +N_e \left(S_i + \sum_{k < i} C_{ik}^{de} + \sum_{k > i} C_{ik}^{ex} \right) + \sum_{k < i} A_{ik} & \text{if } i = j \\ -N_e C_{ij}^{ex} - A_{ji} \frac{f_j}{f_i} & \text{if } i < j, \end{cases} \quad (3)$$

$$b_i^0 = \frac{N_e \alpha_i^{3b} + \alpha_i^{rr}}{f_i}, \quad (4)$$

$$b_i^1 = C_{i1}^{de}. \quad (5)$$

ρ_i is the population of the i th state normalized to that in the Saha equilibrium:

$$\rho_i = \frac{N_i^q}{N_i^E}, \quad (6)$$

$$N_i^E = N_e N_i^{q+1} f_i, \quad (7)$$

$$f_i = 1.64 \times 10^{-22} \frac{g_i}{g^{q+1}} T_e^{-3/2} \exp(E_i/T_e), \quad (8)$$

where g_i is the statistical weight, E_i the ionization energy in eV, and T_e the electron temperature in eV. The matrix inversion of Eq. (2) gives the populations of the excited states in terms of the population of the ground state

$$\vec{\rho} = \vec{r}^0 + N_e \vec{r}^1 \rho_1. \quad (9)$$

The insertion of Eq. (9) into Eq. (1) for the ground state ($i=1$) defines the CR ionization and recombination rate coefficients, respectively, as

$$\begin{aligned} \frac{d}{dt}N_1^q = & -N_e N_1^q \left[S_1 + \sum_{j > 1} \left(C_{1j}^{ex} - r_j^1 \frac{f_j}{f_1} (N_e C_{j1}^{de} + A_{j1}) \right) \right] \\ & + N_e N_1^{q+1} \left[N_e \alpha_1^{3b} + \alpha_1^{rr} + \sum_{j > 1} f_j r_j^0 (N_e C_{j1}^{de} + A_{j1}) \right] \\ \equiv & -N_e N_1^q S^{\text{CR}} + N_e N_1^{q+1} \alpha^{\text{CR}}. \end{aligned} \quad (10)$$

With these CR ionization (S^{CR}) and recombination (α^{CR}) rate coefficients for the ground states which take into account contributions from excited states, the ground state population densities are readily calculated along with evolution of plasma hydrodynamics. Since $\sum_{i>1} N_i^q < N_1^{q+1}$ is satisfied under the QSS approximation [12], the sum of all the ground state population densities can be approximated to the total ion density. Thus the ground state populations can effectively represent the ionization balance.

For the calculation of the CR rate coefficients, the structure of the energy states is required, which is often complex for multielectron ions. However, since the CR rate coefficients are total quantities produced by multistep processes between internal states, they are not so sensitive to the detailed ionic structure of the energy states. As an approximation, the screened hydrogenic model [13] has been already used in the calculation of the ionization balance of complex atom such as selenium [11]. The results were shown to be in good agreement with the calculations where the detailed structure of energy states were used. In this paper the screened hydrogenic model is used to describe the energy states.

In this model, the energy of a state is described by a principal quantum number n with an effective charge Q_n

$$Q_n = Z - \left[\sum_{m < n} \sigma_{nm} P_m + \frac{1}{2} \sigma_{nn} (P_n - 1) \right], \quad (11)$$

where Z is the nucleus charge, σ_{nm} , the screening factor [13] which describes the screening of charge seen by electrons in the n shell by an electron in the m shell, and P_n , the number of electrons in the n shell for a given electron configuration. When only a single excitation is considered, the ionization energy can be written as

$$E_n = 13.6 \frac{Q_n^2}{n^2} \left(1 - \frac{\sigma_{nn}}{Q_n} (P_n - 1) \right) \quad [\text{eV}]. \quad (12)$$

The first term is an attractive potential due to the net ionic charge and the second term is repulsive potential due to the electron in the same shell.

III. CHARACTERISTICS OF THE COLLISIONAL-RADIATIVE RATE COEFFICIENTS

The CR rate coefficients calculated for the ground states of carbon ions including excited states up to $n=20$ are plotted in Fig. 1. Even when the excited states up to $n=100$ were included, the results were the same within the range of 0.1%. In our calculation, excited states up to $n=20$ were used to minimize the computational time. In the region of a low electron density, both the CR ionization and recombination rate coefficients become independent of the electron density. However, note that the CR ionization rate coefficients approach those without the contribution from excited states but the CR recombination rate coefficient does not, indicating that there is still a significant contribution from the excited states even at low electron density. As an electron density increases, S^{CR} also increases but becomes saturated while α^{CR} increases linearly with N_e . The change of the CR rate coefficients due to the contribution from excited states is larger for a lower electron temperature.

This behavior of the CR rate coefficients is better understood by examining them analytically in limiting cases. In the limit of $N_e \rightarrow 0$, electron-collisional processes become slow and the populations of the excited states are determined by the balance between collisional excitation processes from a ground state and radiative decay processes. Hence the rate equations for excited states ($i > 1$) [i.e., Eq. (2)] become

$$\begin{aligned} N_i A_{i1} + \sum_{j=2}^{j=i-1} N_i A_{ij} - \sum_{j=i+1} N_j A_{ji} \\ = N_e N^+ \alpha_i^{\text{rr}} + N_e N_1 C_{1i} \quad (i > 1). \end{aligned} \quad (13)$$

The summation of Eq. (13) over $i (i > 1)$ leads to

$$\sum_{i>1} N_i A_{i1} = N_e N^+ \sum_{i>1} \alpha_i^{\text{rr}} + N_e N_1 \sum_{i>1} C_{1i}, \quad (14)$$

which is then inserted into Eq. (1) for the ground state ($i = 1$), resulting in

$$\frac{d}{dt} N_1 = -N_e N_1 S_1 + N_e N^+ \sum_{i=1} \alpha_i^{\text{rr}}. \quad (15)$$

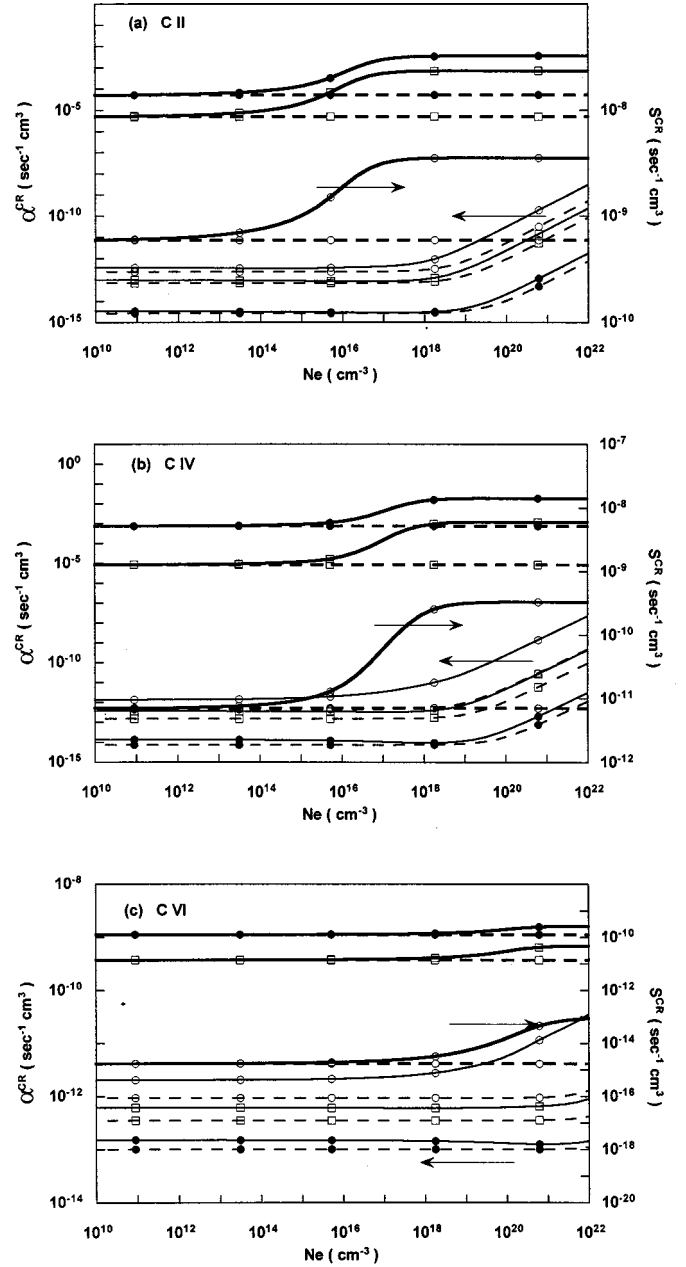


FIG. 1. CR ionization rate coefficients (S^{CR} , thick lines) and recombination rate coefficients (α^{CR} , thin lines) for carbon ions plotted as a function of electron density (N_e) at $T_e = 10$ (○), 46.4 (□), and 1000 eV (●) for (a) C II, (b) C IV, and at $T_e = 46.4$ (○), 215.4 (□), and 1000 eV (●) for (c) C VI. The CR rate coefficients without the contribution from excited states (dashed lines) are also plotted for comparison.

This implies that the electron-collisional excitations from the ground state to the excited states make negligible contributions to the effective ionization process in the region of a low electron density. But in the case of recombination, the excited states still make contributions via the radiative recombination followed by radiative cascades. The effective recombination rate coefficient then becomes the sum of individual radiative recombination rate coefficients. The other limit where $N_e \rightarrow \infty$ can be analyzed using LTE (local thermodynamic equilibrium) model. In this model, the solutions of Eq. (2) are simply $\rho_i = 1 (i > 1)$. Equation (1) for $i = 1$ can be then written as

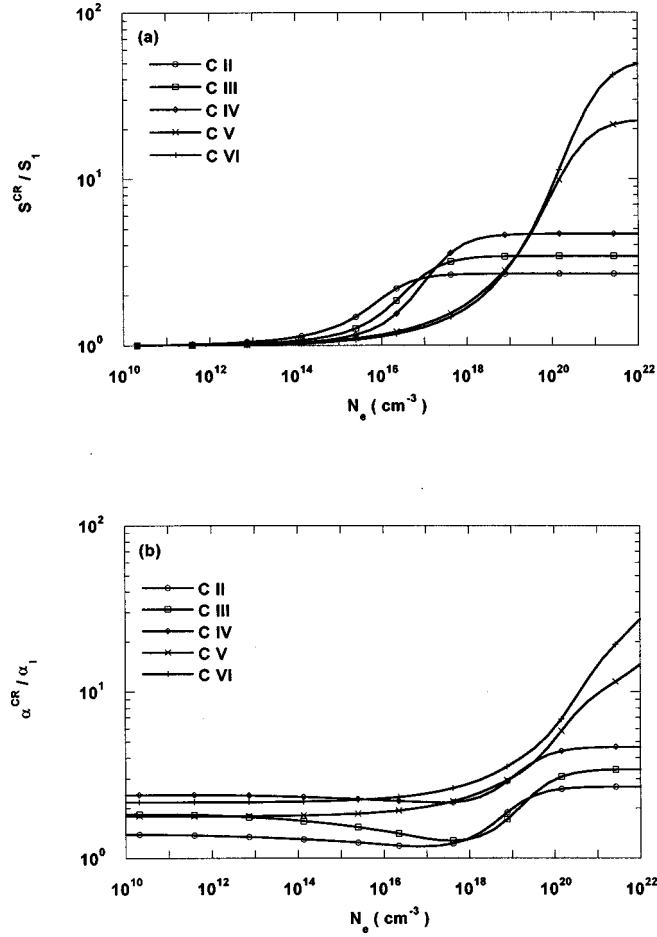


FIG. 2. Ratios of the CR rate coefficients to those without the contribution from excited states are plotted as a function of N_e at $T_e = 46.4$ eV for (a) ionization and (b) recombination.

$$\begin{aligned} \frac{d}{dt} N_1 = & -N_e N_1 \left[S_1 + \sum_{i>1} C_{1i}^{ex} \right] \\ & + N_e N^+ \left[N_e \left(\alpha_1^{3b} + \sum_{i>1} f_i C_{i1}^{de} \right) \right]. \end{aligned} \quad (16)$$

This shows that the CR ionization rate coefficient is given by the sum of the direct ground-to-ground collisional ionization and the collisional excitation rate coefficients from the ground state. The latter will be quickly saturated because the collisional excitation rate coefficient is exponentially decreasing as the energy differences between states become larger. However, note that the CR recombination rate coefficient, consisting of the three-body recombination rate coefficient and the sum of the collisional deexcitation rate coefficients multiplied by f_i , increases linearly with N_e .

The enhancement of the ionization and recombination rate coefficients of the ground states, i.e., the ratios of the CR rate coefficients to direct ground-to-ground rate coefficients are shown in Fig. 2 for various ionization stages at a given temperature of $T_e = 46.4$ eV. The ratios are saturated at different N_e 's for different ionization stages. This saturation can be attributed to the dominance of collisional processes over radiative processes beyond a certain electron density (saturation density). For the CR ionization rate coefficient S^{CR} ,

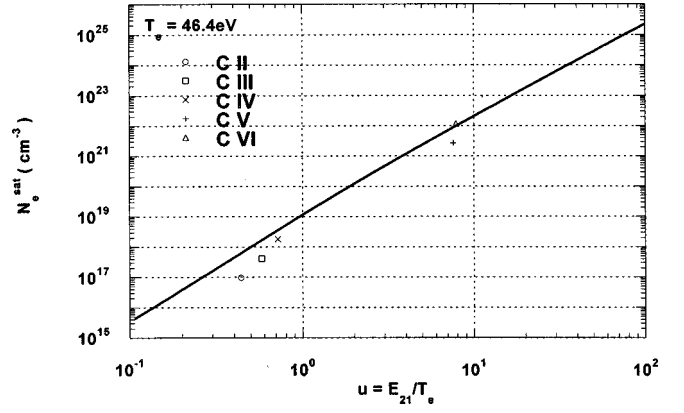


FIG. 3. Saturation electron density N_e^{sat} [Eq. (17)] at which the CR rate coefficients begin to be saturated plotted as a function of $u = E_{21}/T_e$. The saturation densities for different ionization stages obtained from simulations are also shown.

when an electron density is high so that $N_e C_{j1}^{de} \gg A_{j1}$, from Eqs. (2), (3), and (9), one can show that $r_j^1 \propto 1/N_e$. This implies that the terms representing the contribution from excited states become independent of N_e but dependent upon T_e only. The saturation point N_e^{sat} can be estimated by putting $N_e^{\text{sat}} C_{21}^{de} \approx A_{21}$, so

$$N_e^{\text{sat}} \approx \frac{A_{21}}{C_{21}^{de}} = 10^{13} \frac{T_e^{3.5} u^3}{e^u \psi_2(u)} \text{ cm}^{-3}, \quad (17)$$

where $u = \Delta E_{21}/T_e$ and ψ_2 is a function defined in Ref. [14]. For $T_e = 46.4$ eV, Eq. (17) for N_e^{sat} is plotted as a function of u in Fig. 3. N_e^{sat} for different ionization stages obtained from the simulation results are also marked, showing a good agreement with the estimation by Eq. (17). N_e^{sat} was chosen from the simulation data as the density where the ratio becomes 90% of its saturated value. A similar argument holds true for the CR recombination rate coefficients. In this case, the saturation occurs in the electron density region when both the three body recombination and collisional deexcitation processes are larger than the corresponding radiative recombination and spontaneous emission processes, respectively. This condition requires higher density in general.

Another interesting feature in N_e dependence is the negative slope of $\alpha^{\text{CR}}/\alpha_1$ for lower ionization stages near $N_e = 10^{17} \text{ cm}^{-3}$, as manifested in Fig. 2(b). To understand this behavior better, a simple two-level ion is analyzed. One can derive the following relation for $\alpha^{\text{CR}}/\alpha_1$:

$$\begin{aligned} \frac{\alpha^{\text{CR}}}{\alpha_1} - 1 &= \left[\frac{N_e \alpha_2^{3b} + \alpha_2^{rr}}{N_e \alpha_1^{3b} + \alpha_1^{rr}} \right] \left[\frac{N_e C_{21}^{de} + A_{21}}{N_e (S_2 + C_{21}^{de}) + A_{21}} \right] \\ &\equiv P(N_e, T_e) Q(N_e, T_e), \end{aligned} \quad (18)$$

where we note that $P(N_e, T_e)$ includes the recombination process only. Then

$$\frac{d}{dN_e} \left(\frac{\alpha^{\text{CR}}}{\alpha_1} - 1 \right) = \frac{dP}{dN_e} Q + P \frac{dQ}{dN_e}, \quad (19)$$

where

$$\frac{dP}{dN_e} = \frac{\alpha_1^{3b} \alpha_1^{rr}}{[N_e \alpha_1^{3b} + \alpha_1^{rr}]^2} \left[\frac{\alpha_2^{3b}}{\alpha_1^{3b}} - \frac{\alpha_2^{rr}}{\alpha_1^{rr}} \right] > 0 \quad (20)$$

and

$$\frac{dQ}{dN_e} = - \frac{S_2 A_{21}}{[N_e (S_2 + C_{21}^{de}) + A_{21}]^2} < 0. \quad (21)$$

dP/dN_e is always positive because $\alpha_2^{3b} > \alpha_1^{3b}$ and $\alpha_2^{rr} < \alpha_1^{rr}$. Hence the first and second terms in Eq. (19) have different signs. This represents the competition between the recombination to and the collisional ionization from excited states. The electron density and the ratio of temperature to ionization energy in a specific situation determines the sign of Eq. (19). In the case for C II, C III, and C IV in Fig. 2(b), where the electron temperature is in proximity of ionization energies, as the density gets smaller, the recombination also decreases but the density is still high enough for significant collisional excitation and ionization from excited states to occur so that the recombination is effectively hindered. Otherwise the recombination rate coefficient could have been higher. As the density gets decreased further, the collisional processes become much weaker and the recombination now even increases slightly. However, in the case for higher ionization stage such as C V and C VI, where an electron temperature of 46.4 eV is much smaller than their ionization energies, the recombination process compared to collisional process becomes far more dominant than in the case of low ionization stages so that α^{CR}/α does not have a dip but monotonically decreases.

The enhancements of both ionization and recombination rate coefficients of the ground states due to the contribution from excited states become equal to each other when the CR rate coefficients are saturated at high density: for example, for C III $S^{CR}/S_1 = \alpha^{CR}/\alpha_1 = 3.5$ at $N_e = 10^{20} \text{ cm}^{-3}$ and $T_e = 46.4 \text{ eV}$. This can be seen from Eq. (16) through the detailed balancing

$$\begin{aligned} f_1 S_1 &= \alpha_1^{3b}, \\ f_1 C_{i1}^{ex} &= f_i C_{i1}^{de}. \end{aligned} \quad (22)$$

For the C V and C VI ions, there is still a discrepancy between S^{CR}/S_1 and α^{CR}/α_1 , as also shown in Fig. 4, because the saturation density is around $N_e = 10^{24} \text{ cm}^{-3}$ for a given temperature of 46.4 eV. Figure 4 is the variation of S^{CR}/S_1 and α^{CR}/α_1 for C VI at $N_e = 10^{22} \text{ cm}^{-3}$ with respect to temperature, showing the strong dependence of the enhancement on temperature especially in the region of a low temperature. The change of temperature by one order of magnitude from 100 to 10 eV results in the change of 4 orders of magnitude of the CR rate coefficients. The temperature behavior of $\alpha^{CR}/\alpha_1^{3b}$ can be approximately described as

$$\frac{\alpha^{CR}}{\alpha_1^{3b}} \approx \sum_i 14.57 f_{i1} \frac{E_1^2}{(E_1 - E_i)} \frac{\exp(E_i/T_e)}{T_e}, \quad (23)$$

where E_i is the ionization energy of the i th state. The least-square fitting of S^{CR}/S_1 to

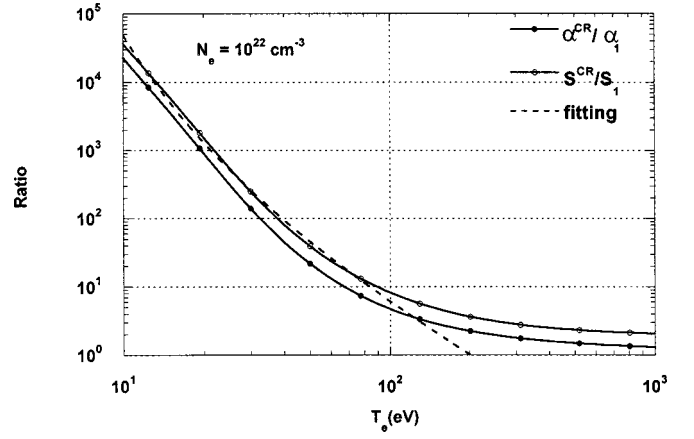


FIG. 4. Ratios of the CR rate coefficients to those without the contribution from excited states are plotted as a function of T_e at $N_e = 10^{22} \text{ cm}^{-3}$ for ionization and recombination for the C VI ion. The least-squares fitting of Eq. (24) is also shown.

$$A \frac{\exp(B/T_e)}{T_e^C}. \quad (24)$$

in the low temperature region of $T_e \leq 100 \text{ eV}$ yields $B \cong 40.5 \text{ eV}$ and $C \cong 2.3$. This implies that the contribution from excited states must be considered in the calculation of the evolution of ionization balance of the low-temperature and high density plasma.

IV. APPLICATION TO GAIN DYNAMICS OF C VI H $_{\alpha}$ IN A RECOMBINING CARBON PLASMA

In the research of x-ray laser using the electron-collisional recombination pumping scheme, one has to treat the evolution of ionization balance in a recombining high-density, low-temperature plasma. To obtain a significant population inversion using the recombination scheme, the cooling process which follows the production of a high-temperature and high-density plasma should be faster than the recombination process. Hence the knowledge of how the ionization balance evolves in a high-density plasma in a cooling phase becomes important.

The CR rate coefficients, discussed in the previous section, have been applied to study the effect of the contribution from excited states on the ionization balance of a gas-puff Z-pinch carbon plasma and on the gain dynamics. In the case of a carbon plasma, the recombination pumping to H-like C VI $n=3$ state from fully stripped C VII ions leads to a lasing action at 18.2 nm with respect to the $n=2$ state.

In a gas-puff Z-pinch plasma, the adiabatic expansion can be considered as a main cooling process which leads to a supercooled plasma [7]. Since the cooling rate is related to the rise time of a plasma current, to know the increase of recombination rate due to the effect by excited states is important for the design of an experimental device.

To observe the effect of excited states on the gain dynamics through the CR rate coefficients, a series of simulations was performed on a Z-pinch carbon plasma using one dimensional MHD (magnetohydrodynamic) code equipped with atomic kinetics. Since the detailed description on this code has been already given in Ref. [7], only a brief expla-

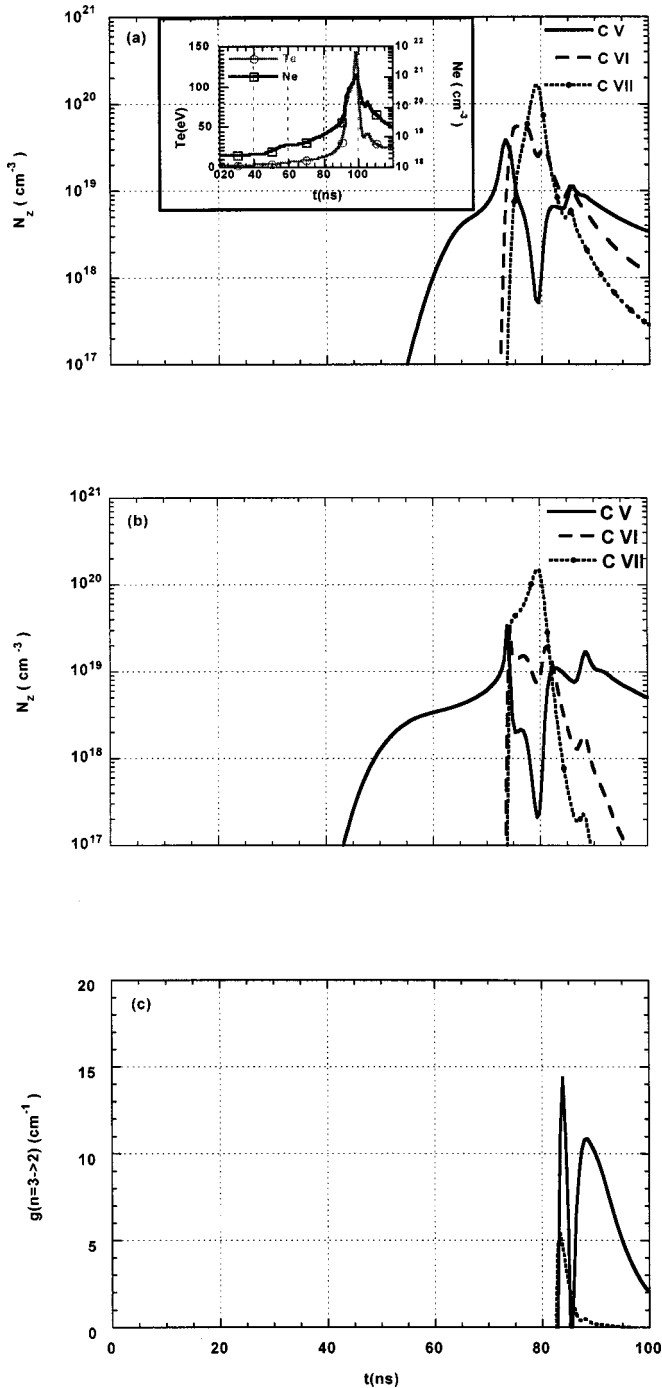


FIG. 5. Temporal changes of carbon ion species calculated from the ionization balance equation: (a) only direct ground-to-ground rate coefficients are used and (b) the CR rate coefficients are used. T_e and N_e are shown in an inset. (c) The gains of C VI H_α (18.2 nm) line are compared without the contribution from excited states (solid line) and with it (dashed line).

nation will be given here. The one-dimensional MHD code solves a single-fluid, two-temperature MHD equation along with an ionization-balance equation, in which the CR rate coefficients or the direct ground-to-ground rate coefficients can be used for the evolution of the ground state populations. The MHD equation includes Joule heating, shock heating, Bremsstrahlung radiation loss, heat conduction, magnetic field diffusion, and shock pressure. The atomic kinetic code evaluates Eq. (1) in a QSS approximation to obtain the ex-

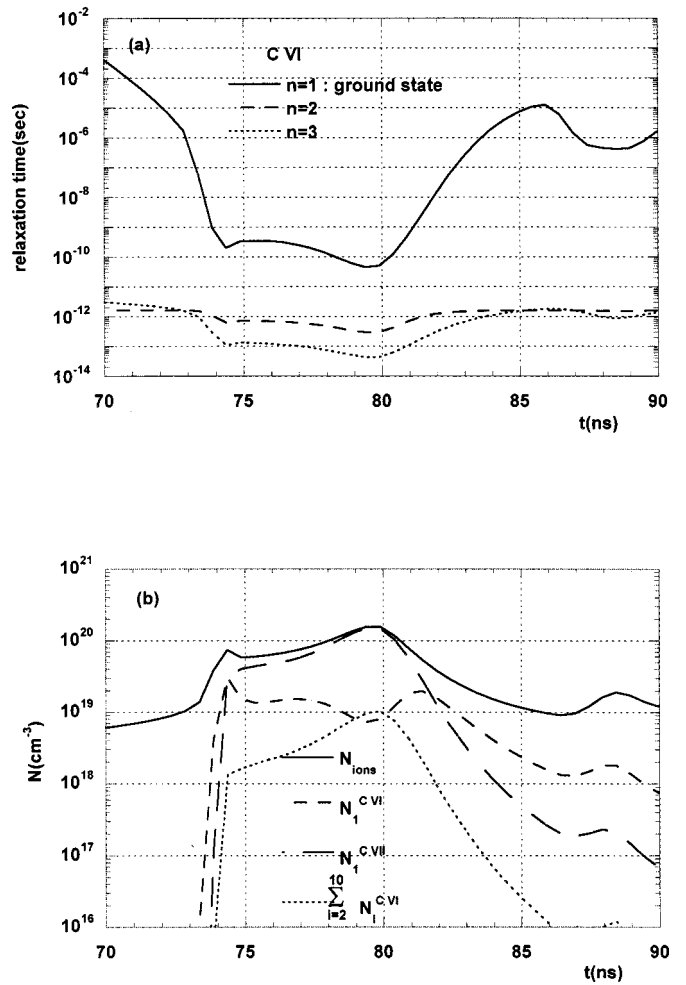


FIG. 6. (a) Relaxation times of the ground and excited states of the C VI ion and (b) the populations of the ground states of C VII, C VI ion, and the sum of the excited level populations. The total ion density is also plotted for comparison.

cited state populations as a post processor to the MHD code. The radiative reabsorption is also included. Figure 5 show the temporal changes of the ground state populations of C V, C VI, and C VII ions. Figure 5(a) is the case where the direct ground-to-ground rates (no contribution from excited states) are used and Fig. 5(b) the case where the CR rates are used. The corresponding T_e and N_e are shown in an inset. This was obtained for a Z-pinch carbon plasma of the initial density of $2.5 \times 10^{18} \text{ cm}^{-3}$ with the quarter period of a driving current pulse being 100 ns and a peak plasma current 110 kA. The initial plasma radius was set to be 2 mm. The effect on the evolution of the ionization balance is manifested by the fact that C VII ions depletes much faster (~ 5 ns) than in the case of only the direct ground-to-ground processes being included (~ 20 ns). This is a significant change in the point of the pumping time scale requirement. The time scale of temperature change is about ~ 5 ns, which is comparable with the recombination time of ~ 1 ns [Fig. 1(c)]. But the rapid depletion of C VII ions implies the reduction in the pumping source for the upper lasing state ($n=3$) at an adequate condition for the gain. The gain is thus much reduced (by factor of 3) and exists for a shorter duration [Fig. 5(c)].

The role of the increased recombination rate of C VI to C V ion should be also noticed. When only the CR rates

between C VII and C VI ion are included, no gain was observed. In this case, the slow depletion of C VI ions results in populating the low lasing state ($n=2$) through the electron-collisional excitation and reabsorption process. Thus the increase of the recombination rate from C VI to C V ion has positive effect on the gain dynamics through effectively lowering the population of the $n=2$ state. This demonstrates the importance of the consistent inclusion of the contribution from excited states in the ionization and recombination rate coefficients for all ionization stages.

Up to now, the QSS approximation has been used. For the QSS to be valid, the following two conditions [12] are to be met. One is the relaxation time requirement which has already been discussed in Sec. II. The relaxation times of the ground state and the excited levels for C VI ion, which are most relevant to the recombination process under interest, are shown for the plasma discussed in this section in Fig. 6(a). The relaxation time of the ground state is seen to be longer than those of the excited states by two orders of magnitude. Hence the relaxation time requirement is well satisfied. The other condition, expressed by the inequality

$$\sum_{i>1} N_i^q < N_1^{q+1}. \quad (25)$$

is also checked by comparing the population density of C VII ion and the sum of the excited level populations of the C VI ion [Fig. 6(b)]. The summation is done over up to principal quantum number, $n=10$ taking into account continuum lowering [13]. This also shows that the plasma under interest is well in the region of the QSS approximation. Since the sum of all the ground state populations is approximated to the total ion density from Eq. (25), this introduces an error of less than 10% in the ground state population of an ion stage with respect to its total ion density in the evaluation of ionization balance but it does not change our conclusion and the gain characteristics.

V. CONCLUSIONS

The effect of excited states on the CR ionization and recombination rate coefficients has been studied, especially for carbon ions in view of their importance of x-ray laser development at 18.2 nm. The collisional-radiative ionization and recombination rate coefficients for the ground states of carbon ions were calculated using the screened hydrogenic atomic model and characterized. The calculations can be done for other ions. The characteristics for carbon ions are generic and applicable to other ions.

The results reveal that the contribution from excited states begins to play an important role from the electron density as low as $N_e \approx 10^{15} \text{ cm}^{-3}$ and becomes saturated at $N_e \approx 10^{20} \text{ cm}^{-3}$. In the case of recombination, due to the radiative process from the higher ionization stage to excited states, the CR recombination rate coefficient is higher than the direct ground-to-ground recombination rate coefficient even at low electron densities (as low as 10^{10} cm^{-3}), where the contribution from excited states has been considered to be negligible. The contribution enhances the rate coefficients by several orders of magnitude at a high electron density and specially at a low electron temperature.

Some of these characteristics were understood analytically in the asymptotic cases of $N_e \rightarrow 0$ and $N_e \rightarrow \infty$. These analytic formulas can be directly applied to a plasma in corona regime and LTE regime.

The effect on the gain of C VI H_α (18.2 nm) line during the course of the evolution of a Z-pinch carbon plasma was investigated. This study reveals the increased recombination rate in the cooling phase significantly shorten the lifetime of C VII ions, making the gain both short lived and smaller.

ACKNOWLEDGMENTS

This work has been supported in part by the POSTECH/BSRI special fund, the Basic Science Research Institute Program, Ministry of Education (Project No. BSRI-98-2439), and KOSEF (Contract No. 951-0205-017-2).

-
- [1] J. Quant. Spectrosc. Radiat. Transf. **58**, 399 (1997).
 - [2] R. C. Elton, *X-ray Lasers* (Academic, New York, 1990), Chap. 4.
 - [3] S. Suckewer, C. H. Skinner, H. Milchberg, C. Keane, and D. Voorhees, Phys. Rev. Lett. **55**, 1753 (1985); D. V. Korobkin, C. H. Nam, S. Suckewer, and A. Golstov, *ibid.* **77**, 5206 (1996); D. Korobkin, A. Golstov, A. Morozov, and S. Suckewer, *ibid.* **81**, 1607 (1998).
 - [4] D. Kim, C. H. Skinner, A. Wouters, E. Valeo, D. Voorhees, and S. Suckewer, J. Opt. Soc. Am. B **6**, 115 (1989).
 - [5] D. Kim, C. H. Skinner, G. Umesh, and S. Suckewer, Opt. Lett. **14**, 665 (1989).
 - [6] Hyun-Joon Shin, Dong-Eon Kim, and Tong-Nyong Lee, Phys. Rev. E **50**, 1376 (1994).
 - [7] K. T. Lee, S. H. Kim, D. Kim, and T. N. Lee, Phys. Plasmas **3**, 1340 (1996).
 - [8] D. B. Graves, IEEE Trans. Plasma Sci. **22**, 31 (1994).
 - [9] C.-H. J. Wu, M. Meyyappan, and D. J. Economou, IEEE Trans. Plasma Sci. **23**, 503 (1995).
 - [10] D. R. Bates, F. R. S., A. E. Kingston, and R. W. P. McWhirter, Proc. R. Soc. London, Ser. A **267**, 297 (1962).
 - [11] Y. T. Lee, J. Quant. Spectrosc. Radiat. Transf. **38**, 131 (1987).
 - [12] R. W. P. McWhirter and A. G. Hearn, Proc. Phys. Soc. London **82**, 641 (1963).
 - [13] R. M. More, J. Quant. Spectrosc. Radiat. Transf. **27**, 345 (1982).
 - [14] H. W. Drawin (unpublished).